IEEE Access
Multidisciplinary | Rapid Review | Open Access Journal

Received January 7, 2019, accepted January 10, 2019, date of publication January 22, 2019, date of current version February 12, 2019.

Digital Object Identifier 10.1109/ACCESS.2019.2894259

Multi-Objective Optimization Control of Distributed Electric Drive Vehicles Based on Optimal Torque Distribution

JUHUA HUANG[1], YINGKANG LIU[1], MINGCHUN LIU[1], MING CAO[1], AND QIHAO YAN[2]
[1]School of Mechatronics Engineering, Nanchang University, Nanchang 330031, China
[2]Planning and Financial Affairs Department, Nanchang University, Nanchang 330031, China

Corresponding author: Mingchun Liu (liumingchun@ncu.edu.cn)

This work was supported in part by the National Natural Science Foundation of China under Grant 51605214 and Grant 51762034 and in part by the Natural Science Foundation of Jiangxi Province under Grant 20171BAB216028.

ABSTRACT To improve the total efficiency of the drive system and the driving safety of distributed electric drive vehicles, this paper proposes a multi-objective optimization method based on torque allocation optimization. First, in the vehicle nonlinear dynamics model, the response surface method is used to perform regression analysis on the test data of the drive motor to obtain the drive motor efficiency function. Second, based on the demand torque value of the distributed electric drive system, the objective functions that characterize the optimization of the drive system efficiency and the optimization of the vehicle driving safety are established. Moreover, the linear weighting method with adaptive weight coefficients is used to transform the solution of the above two objective functions into a multi-objective optimization problem under constraint conditions. Furthermore, the second-generation nondominated sorting genetic algorithm (NSGA-II) and the hybrid genetic Tabu search algorithm (HGTSA) are used to solve the above multi-objective optimization problem to obtain the optimal torque distribution of the distributed electric drive system. Finally, the NEDC operating conditions were selected to verify NSGA-II, the HGTSA and the commonly used average distribution method. The simulation test results show that NSGA-II and the HGTSA can improve the driving efficiency and vehicle driving safety of distributed electric drive systems relative to the average distribution method. In particular, the optimization effect of the HGTSA is more prominent, and stability is more quickly achieved.

INDEX TERMS Multi-objective optimization, NSGA-II, Tabu search, torque distribution.

I. INTRODUCTION

With energy conservation and environmental protection becoming the theme of modern times, the development of electric vehicles has entered a new era [1], [2]. Hybrid electric vehicles and pure vehicles have become areas of active research [3], mainly involving the study of batteries and engines in the field of pure electric vehicles. Energy management is the main research direction of hybrid vehicles [4], [5]. However, there are few studies on vehicle dynamics control. Pure electric vehicles rely on the drive system to meet driving needs, and the quality of the drive system has a great impact on the performance of the entire vehicle. There are two types of electric vehicle driving methods: centralized driving and distributed driving. The distributed electric drive vehicle does not require mechanical transmission components, which improves the space utilization efficiency of the entire vehicle. Most importantly, this vehicle breaks the fixed-torque distribution mode of the traditional vehicle and arbitrarily distributes the wheel torque to driving motor according to the actual road conditions and the driving state of the vehicle. Although distributed electric drive vehicles have many advantages as described above, they also face an urgent problem that needs to be solved: how to reasonably distribute the demand torque into each drive wheel to improve the efficiency, the driving safety and the steering stability of the entire vehicle drive system.

The driving motor is the only power source on the pure electric vehicle, and its performance directly affects the economy and power of the electric vehicle. To improve the working efficiency of the drive motor and make it work in the

high-efficiency range as much as possible, the single-motor-drive vehicle mainly adopts the economic shift schedule in advance and then applies this rule to the vehicle model to carry out the standard working condition simulation experiment. According to the results, the pre-established shifting rules are corrected to obtain the final economic shifting curve [6]. This method improves the working efficiency of the motor to a certain extent, but the predetermined shifting rules are too complex and are not applicable to general working conditions. Multimotor driven vehicles have the advantage of independently controlling driving and braking torque. Moreover, the wheel torque can be arbitrarily distributed according to the actual road working conditions and the running state of the vehicle, thereby realizing the control of the longitudinal dynamic safety and energy saving of the electric vehicle. At present, multimotor driven vehicles optimize the torque distribution to improve the motor working efficiency by the following three methods: drawing the motor efficiency map according to the motor data, using the polynomial fitting method to obtain the motor efficiency function and establishing the driving motor loss model.

Scholars have obtained the map of motor speed, demand torque and motor efficiency and have adopted the off-line optimization calculation method to obtain the front-axle torque distribution coefficient of the drive system change with the motor speed and demand torque. Furthermore, the two-dimensional lookup-table method is used to optimize the torque distribution and carry out the standard working condition simulation experiment. It is concluded that when the demand torque of the vehicle is small, a single-axis drive should be used; when the demand torque is large, four-wheel drive is better. Optimizing torque distribution according to the motor efficiency map can reduce energy consumption to a certain extent but requires accurate motor data for support. Moreover, the accuracy of the front-axle torque distribution coefficient depends heavily on the difference method used to plot the motor efficiency map [7]–[9]. Chen *et al.* [10], [11] obtained a simplified relationship between motor efficiency and demand torque by fitting the motor data, but they did not consider the influence of wheel speed, resulting in unreasonable torque distribution under certain operating conditions. Some scholars [12], [13] have proposed to establish a drive motor loss model for distributed electric drive vehicles to improve motor drive efficiency. The results show that the highest drive system efficiency can be obtained by using the torque average distribution method under straight-line driving conditions. However, this approach does not consider the motion state of the vehicle because the acceleration of the vehicle has a great influence on the drive mode switching. In terms of longitudinal dynamics safety control, many scholars have conducted a significant number of research studies. Hartani *et al.* [14] considered the difference between the front and rear wheelbases of the vehicle and found that the wheel load changes with the longitudinal acceleration of the body. Therefore, an optimized torque distribution strategy based on the load ratio is proposed. Although the load-based proportional distribution strategy can adjust the torque assigned to the drive wheels in real time according to the wheel load change, the adhesion limit of the tire is neglected, resulting in slipping or skidding of the tire when the vehicle speed is higher [15]. Lu *et al.* [16] and Xiong *et al.* [17] used hierarchical control to optimize torque distribution. These researchers took the minimum sum of the tire load rate as the objective function and proposed a linear quadratic regulator with gaining, and then, they used the weighted quadratic programming method to optimize the demand torque. The results showed that the longitudinal force output reserve of the tire can be greatly improved, thereby improving the longitudinal driving safety of the vehicle.

However, these scholars considered only the torque distribution under the single objective function. While distributed electric drive vehicles are a highly complex coupled nonlinear time-varying system, the torque optimization distribution control strategy should consider multiple objective functions to meet various vehicle performance metrics. Considering the efficiency of the driving system of the vehicle and the driving safety, De Novellis *et al.* [18] proposed four objective functions: the minimization of the overall input motor power, the minimization of the standard deviation of longitudinal tire slip with respect to the average slip of the four wheels, the minimization of the total longitudinal slip power loss, and the minimization of the sum of the tire force coefficients. However, the authors do not consider the four objective functions to be integrated into the torque distribution and do not provide the online optimization method. Guo *et al.* [19] considered three objective functions: energy consumption, tire utilization and torque variation. These researchers set the wheel speed to a constant value to obtain the motor efficiency as a function of demand torque. In addition, the weight coefficients of the three objective functions are fixed values, which makes it impossible to adjust the priority of the objective function in real time according to the road conditions to optimize the effect of torque distribution.

At present, there are many algorithms for dealing with multi-objective optimization problems: the model predictive control (MPC) algorithm, dynamic programming (DP) algorithm, multi-objective genetic algorithm (NSGA), multi-objective particle swarm optimization (MOPSO) [20], multi-objective evolutionary algorithm (MOEA) [21] and so on. In [22], the MPC algorithm is used to obtain the optimal solution under three objective functions. However, if the gradient and the Hessian matrix of the objective function are too complex, the computational burden of the MPC will increase, and the simulation time will be prolonged. In [19], the improved particle swarm optimization (APSO) algorithm for optimizing torque distribution was shown to achieve ideal results, but it satisfies the accuracy requirement at the expense of increased computation time. In [23], the second generation nondominated sorting genetic algorithm (NSGA-II) was used to address multi-objective optimization problems, and the output from the five standard-difficulty test problems was compared with that of PAES and SPEA, two other

multi-objective optimization algorithms. The results showed that in most problems, NSGA-II can find the optimal solution near the Pareto frontier, and the convergence effect is better. According to these studies, the demand torque can be allocated to the driving wheels through the optimization algorithm under various constraints to improve the driving system efficiency and driving safety. However, the different road conditions of the vehicle cause the priority of the objective function to change in real-time as well.

To improve the efficiency of the drive system and the longitudinal driving safety of distributed drive vehicles, this paper presents the following work. First, in the vehicle nonlinear dynamics model, the response surface method is used to perform regression analysis on the test data of the drive motor to obtain the drive motor efficiency function. Second, based on the demand torque value of the distributed electric drive system, the objective functions that characterize the efficiency optimization of the drive system and the optimization of the driving safety of the vehicle are established. The linear weighting method with adaptive weight coefficient is used to transform the solution of the above two objective functions into a multi-objective optimization problem that can adjust the priority of the objective function in real time according to road conditions and vehicle body state under constraint conditions. Furthermore, NSGA-II and the hybrid genetic tabu search algorithm (HGTSA) are used to solve the above multi-objective optimization problem to obtain the optimal torque distribution of the distributed electric drive system. Finally, using NEDC working conditions, NSGA-II, the HGTSA and commonly used average distribution methods are compared and verified on the MATLAB/Simulink software platform.

The structure of this paper is as follows. Vehicle dynamics modeling and motor efficiency function modeling are presented in the second section. The third section proposes a multi-objective optimization algorithm based on torque allocation optimization. The fourth section selects the NEDC operating conditions for simulation experiments. The study's conclusions are presented in the fifth section.

II. ESTABLISHING THE MODEL

A. VEHICLE DYNAMIC MODELING

To comprehensively study the kinematic characteristics of the vehicle, the magic formula tire model [24] was selected. A seven-degree-of-freedom vehicle model, as shown in Fig. 1, was established, including three degrees of freedom of the longitudinal, lateral and yaw of the vehicle body and the rotational degrees of freedom of the four wheels.

Where u, v, and ω_r represent the vehicle longitudinal velocity, lateral velocity, and yaw rate, respectively. δ_{fl} is the front wheel angle. a and b represent the distance from the front axle and rear axle to the center of gravity (C.G.), respectively. l_x is the wheelbase between the left and right wheels. F_{xi} and F_{yi}(i=fl,fr,rl,rr) represent the longitudinal tire force and lateral tire force on the vehicle coordinate frame (o-xyz), respectively.

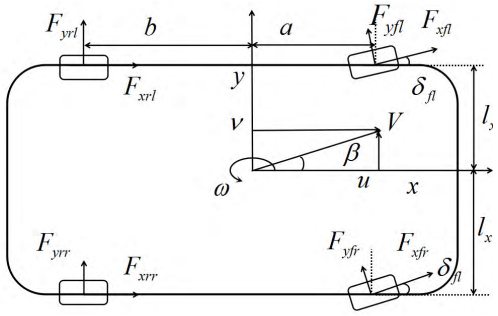

FIGURE 1. Seven-degree-of-freedom vehicle model.

According to Figure 1 and Newton's second law, the dynamics analysis of the vehicle can obtain the balance equation of the longitudinal force, lateral force and yaw torque as follows:

$$m(\dot{u} - v\omega_r) = \left(F_{xfl} + F_{xfr}\right)\cos\delta_{fl} - \left(F_{yfl} + F_{yfr}\right)\sin\delta_{fl} + F_{xrl} + F_{xrr} \quad (1)$$

$$m(n\dot{u} + u\omega_r) = \left(F_{xfl} + F_{xfr}\right)\sin\delta_{fl} + \left(F_{yfl} + F_{yfr}\right)\cos\delta_{fl} + F_{yrl} + F_{yrr} \quad (2)$$

$$\begin{aligned} I_Z\dot{\omega}_r = {} & (F_{xfl}\sin\delta_{fl} + F_{yfl}\cos\delta_{fl})a \\ & - (F_{xfl}\cos\delta_{fl} - F_{yfl}\sin\delta_{fl})\frac{l_x}{2} \\ & + (F_{xfr}\delta_{fl} + F_{ylr}\cos\delta_{fl})a \\ & + (F_{xfr}\cos\delta_{fl} - F_{yfr}\sin\delta_{fl})\frac{l_x}{2} \\ & - (F_{xrl} + F_{xrr})b + (F_{xrr} - F_{xrl})\frac{l_x}{2} \end{aligned} \quad (3)$$

where m is the mass of the entire vehicle. I_z represents the moment of inertia of the vehicle around the Z-axis.

The equation of motion of the wheel is

$$\begin{cases} I_\omega \dot{\omega}_{fl} = T_{dfl} - T_{bfl} - R_W F_{xfl} \\ I_\omega \dot{\omega}_{fr} = T_{dfr} - T_{bfr} - R_W F_{xfr} \\ I_\omega \dot{\omega}_{rl} = T_{drl} - T_{brl} - R_W F_{xrl} \\ I_\omega \dot{\omega}_{rr} = T_{drr} - T_{brr} - R_W F_{xrr} \end{cases} \quad (4)$$

where I_ω represents the wheel inertia. T_{di} and T_{bi} represent the driving torque and braking torque of the four wheels, respectively. R_w is the rolling radius of the wheel.

B. MOTOR EFFICIENCY FUNCTION MODELING

To meet the vehicle performance requirements, the maximum speed is 160 km/h, and the maximum grade is 40%. The motor is selected with a peak torque of 320 Nm and a peak power of 25 kW. The external characteristic curve of each in-wheel motor is shown in Fig. 2:

The map shown in Fig. 3 is drawn based on the motor experiment data.

The motor efficiency can be determined simply by knowing the motor speed and the required torque. Therefore, the response surface method is used to perform regression analysis on the motor data. To obtain an accurate functional

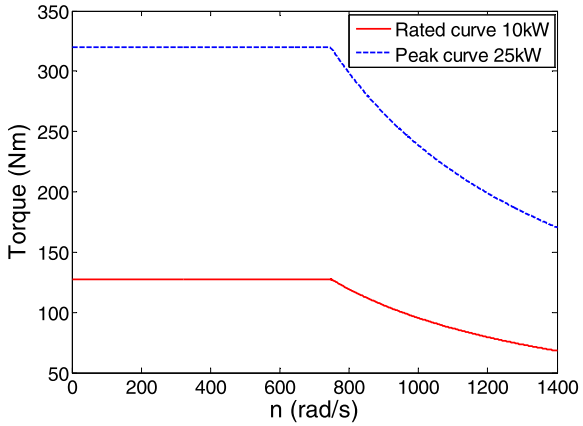

FIGURE 2. Motor external characteristic curve.

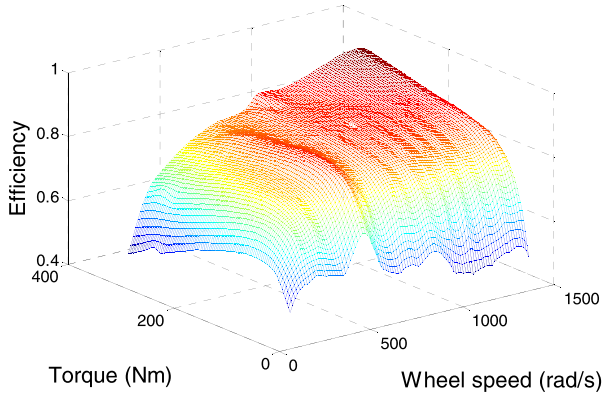

FIGURE 3. Motor efficiency map.

relationship between the response variable and the design variable, the motor efficiency Y is described by a fourth-order regression equation with cross terms [25], which is expressed as follows:

$$Y = \sum_{\substack{i=0 \\ j=0 \\ i+j\leq 4}}^{4} \beta_{ij} x_1^i x_2^j + \varepsilon \tag{5}$$

whereβ is the regression coefficient and x_1 and x_2 represent the design variables: the motor speed and demand torque, respectively. ε is a random error vector.

The response function model can be described in matrix form and written as

$$Y = X\beta + \varepsilon \tag{6}$$

where X is the design variable combination matrix, β is the regression coefficient matrix, and ε is the random error vector matrix.

The regression coefficient matrix is estimated by the least squares method; that is, the sum of squared errors of equation (6) is minimized.

The least squares function L is

$$L = \sum_{i=1}^{n} \varepsilon_i^2 = \varepsilon'\varepsilon = (Y - X\beta)'(Y - X\beta) \tag{7}$$

where ε' is the transposed matrix of ε.

The least squares function is minimized with respect to the regression coefficient. The least squares estimator $\hat{\beta}$ must satisfy

$$\left.\frac{\partial L}{\partial \beta}\right|_{\hat{\beta}} = -2X'Y + 2X'X\hat{\beta} = 0 \tag{8}$$

Thus, the least squares estimator and the fitted regression model can then be obtained as

$$\hat{\beta} = (X'X)^{-1}X'Y \tag{9}$$

$$\hat{Y} = X\hat{\beta} \tag{10}$$

According to the calculation method of the above formula (5)-(10), the coefficient vector β of the fourth-order regression equation of Y is obtained as

β=[2.4637e-04, 0.0026, 0.0113, 4.4833e-06, 8.94445e-06, 9.2713e-05, 3.2682e-09, 6.6470e-09, 4.5393e-08, 2.9895e-07, 8.5545e-13, -1.7241e-12, 1.3175e-11, 6.4230e-11, 3.4565e-10]

Therefore, the functional relationship between motor efficiency, motor speed, and demand torque can be expressed as

$$\begin{aligned}\eta = {} & 2.4637 * 10^4 + 0.0026\mathrm{n} + 0.0113T - 4.4833 \\ & * 10^6 n^2\text{-}8.94445 * 10^6 n * T - 9.2713 * 10^5 T^2 \\ & + 3.2682 * 10^9 n^3 + 6.6470 * 10^9 n^2 * \mathrm{T} + 4.5393 \\ & * 10^8 n * \mathrm{T}^2 + 2.9895 * 10^7 T^3 - 8.5545 * 10^{13} n^4 \\ & - 1.7241 * 10^{12} n^3 * \text{T-}1.3175 * 10^{11} n^2 \\ & * \mathrm{T}^2 - 6.4230 * 10^{11} n * \mathrm{T}^3 - 3.4565 * 10^{10} \mathrm{T}^4\end{aligned} \tag{11}$$

To test the accuracy of the fourth-order model, the scatter plot of the motor speed, demand torque, and motor efficiency based on the fourth-order function of motor efficiency and the data-based scatter plot are shown in Fig. 4.

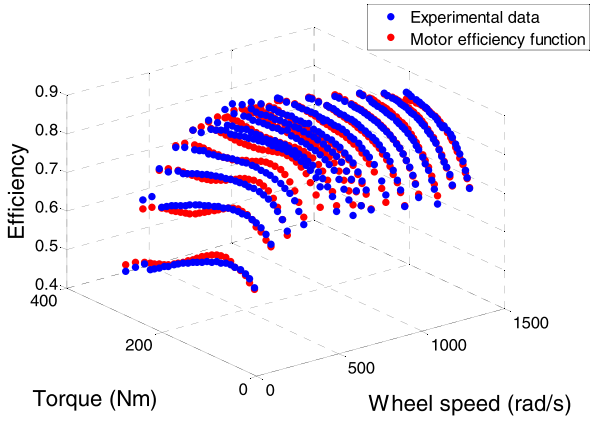

FIGURE 4. Motor efficiency scatter plot.

Equation (11) is used to calculate each estimated value $\hat{Y}$ of the response variables in Figure 4, and the remaining standard deviations can be calculated from

$$S_{Y|1,2,...O} = \sqrt{\sum_{i}^{h} \frac{(Y_i - \hat{Y}_i)^2}{h - o - 1}} \tag{12}$$

where h is the number of motor data point, and o is the number of independent variables. The remaining standard deviation is 0.0208, which shows that the fourth-order motor efficiency function obtained from the regression analysis can well represent the relationship between motor speed, demand torque and motor efficiency.

III. TORQUE OPTIMIZATION ALLOCATION STRATEGY

A. CONTROL STRATEGY

A flowchart of the torque optimization allocation strategy proposed in this paper is shown in Fig. 5.

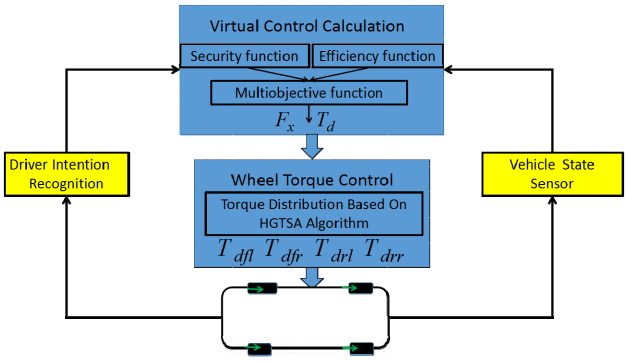

FIGURE 5. Control strategy flowchart.

At the upper level of the controller, the demand torque moment can be calculated from the driver's intention and the vehicle sensor data together with the wheel speed as an input to the torque distribution execution layer. In the lower layer of the controller, objective functions that characterize the optimization of the drive system and the optimization of the driving safety of the vehicle are established. Then, the linear weighting method with adaptive weight coefficient is used to transform the solution of the above two objective functions into a multi-objective optimization problem that can adjust the priority of the objective function in real time according to the road conditions and vehicle body state under constraint conditions. Furthermore, NSGA-II and the HGTSA are used to solve the above multi-objective optimization problem to obtain the optimal torque distribution of the distributed electric drive system. Finally, using NEDC working conditions, NSGA-II, the HGTSA and commonly used average distribution methods are compared and verified on the MATLAB/Simulink software platform.

B. OBJECTIVE FUNCTION

1) DRIVE SYSTEM EFFICIENCY OBJECTIVE FUNCTION

The driving efficiency of the system is equal to the output power divided by the input power.

$$\eta_{System} = \frac{T_d \cdot n}{\frac{T_{dfl} \cdot n_{fl}}{\eta_{fl}} + \frac{T_{dfr} \cdot n_{fr}}{\eta_{fr}} + \frac{T_{drl} \cdot n_{rl}}{\eta_{rl}} + \frac{T_{drr} \cdot n_{rr}}{\eta_{rr}}} \tag{13}$$

To improve the driving efficiency of the system, it is necessary to reduce the input power of the entire vehicle. Therefore, the minimum input power of the vehicle is used as the objective function to characterize the drive system efficiency:

$$J_1 = \min\left(\frac{T_{dfl} \cdot n_{fl}}{\eta_{fl}} + \frac{T_{dfr} \cdot n_{fr}}{\eta_{fr}} + \frac{T_{drl} \cdot n_{rl}}{\eta_{rl}} + \frac{T_{drr} \cdot n_{rr}}{\eta_{rr}}\right) \tag{14}$$

where η_i (i=fl,fr,rl,rr) can be calculated from the motor efficiency function (11).

Assume that the left and right wheel torques and speeds are equal:

$$J_1 = \min\left(\frac{2 \cdot T_{dfl} \cdot n_{fl}}{\eta_{fl}} + \frac{2 \cdot T_{drr} \cdot n_{rr}}{\eta_{rr}}\right) \tag{15}$$

The constraints that correspond to the objective function are

$$\begin{aligned} \sum T_{di} &= T_d \\ T_{\dim in} &\le T_{di} \le T_{\dim ax} \end{aligned} \tag{16}$$

2) DRIVING SAFETY OBJECTIVE FUNCTION

The output reserve of the longitudinal force of the tire can be expressed by the tire load rate γ:

$$\gamma_i = \frac{F_{xi}}{\mu F_{zi}} \quad i = fl, fr, rl, rr \tag{17}$$

where μ is the road surface adhesion coefficient and F_{xi} and F_{zi} represent the longitudinal force and vertical force of each tire, respectively. The longitudinal force can be obtained from the tire torque:

$$F_{xi} = \frac{T_{di}}{R} i = fl, fr, rl, rr \tag{18}$$

When the tire load rate γ is large, the longitudinal force accounts for a larger proportion in the friction ellipse, and the proportion of the lateral force decreases accordingly. When γ =1, the longitudinal force that the tire can provide at this time has reached the adhesion limit, and the lateral force is equal to 0, which means that the vehicle's operational stability and driving safety are relatively poor. Therefore, it is desirable for the tire load rate γ to remain as small as possible to increase the longitudinal force output reserve and the vehicle stability margin. When the tire load rate γ is small, the lateral force margin increased and the driving safety is improved, and the motor input power is small, which can improve the driving efficiency of the vehicle to a certain extent.

Based on this condition, the objective function J_2 that characterizes driving safety is determined as follows:

$$J_2 = \min \sum \gamma_i = \min \sum \frac{T_{di}/R}{\mu F_{zi}} \quad i = fl, fr, rl, rr \tag{19}$$

3) MULTI-OBJECTIVE OPTIMIZATION FUNCTION

Many scholars use the linear weighting method, geometric weighting method, adaptive weight coefficient and other methods to transform the multi-objective optimization problem into a single-objective optimization problem:

$$\begin{cases} \min f(x) \\ S.tx \in X \end{cases} \tag{20}$$

where f(x) is the transformed single-objective function and X is the corresponding constraint.

Because the linear weighting method has the advantages of simplicity and high efficiency, the adaptive weighting coefficient can change the weighting coefficient in real time according to the actual situation to obtain the optimal result. Therefore, this paper uses the linear weighting method with adaptive weight coefficients to transform the above two objective functions into a single-objective optimization function. First, the two objective functions are unified by the max-min normalization method.

$$f_i(x) = \frac{f_i(x)_{\max} - f_i(x)}{f_i(x)_{\max} - f_i(x)_{\min}} \quad i = 1, 2 \tag{21}$$

In the case of low speed and good road conditions, the efficiency of the drive system is improved to obtain satisfactory economical driving performance of the vehicle. However, in the case of high speed or poor road conditions, the safety of the vehicle should be ensured first. The adaptive weight coefficient ω value is a segmentation function of the road surface adhesion coefficient μ and the speed u:

$$\begin{cases} \omega = (\omega_{1\max} - \omega_{1\min}) \cdot \sin(\frac{u}{u_{\max}}) + \omega_{1\min} & if\ 0.7 \le \mu \le 1 \\ \omega = (\omega_{2\max} - \omega_{2\min}) \cdot \sin(\frac{u}{u_{\max}}) + \omega_{2\min} & if\ \mu < 0.7 \end{cases} \tag{22}$$

where $\omega_{1\max}$, $\omega_{1\min}$, $\omega_{2\max \backslash and} \omega_{2\min}$ represent the maximum and minimum of the weighting coefficients of the first objective function on the high-adhesion and low-adhesion road surfaces, respectively.

Thus, the optimized objective function J is

$$J = \omega_1 J_1 + \omega_2 J_2 \tag{23}$$

The corresponding constraints are

$$\begin{aligned} &\sum T_{di} = T_d \\ &T_{\dim ax} \le T_{di} \le T_{\dim ax} \end{aligned} \tag{24}$$

C. OPTIMIZATION ALGORITHM

1) SECOND-GENERATION NONDOMINATED SORTING GENETIC ALGORITHM

This paper studies the nonlinear multi-objective optimization problem with constraints. At present, there are two solutions. One is to use the weight coefficients proposed in the previous section to weight each objective function as a single objective function. The other is to simultaneously optimize multiple target functions to generate a set of Pareto optimal solutions and then determine which solution is optimal.

The nondominated sorting genetic algorithm (NSGA) was originally proposed by Srinivas and Deb [26]. Although it can effectively address multi-objective optimization problems, it also has some disadvantages: computational complexity, lack of elitism and the need to develop shared parameters. To address the deficiencies of the NSGA, Deb *et al.* [23] proposed NSGA-II. The advantages of NSGA-II over NSGA are as follows: fast nondominated sorting operator design, individual crowding distance operator design, and elite strategy selection operator design.

The main steps of NSGA-II are as follows:

a: POPULATION INITIALIZATION

Randomly generate the initial population, set the number of objective functions and variables, and set constraints.

b: NONDOMINATED SORTING

The initialized population is sorted according to nondomination using the following pseudocode.

c: CROWDING DISTANCE

After nondominated sorting, the rank ordering Front_i of each individual is obtained. To perform selective sorting within individuals of the same rank, it is necessary to calculate the crowded distance of the individual. The crowded distance of the individual i is the distance between the two individuals i+1 and i−1 adjacent to i in the target space. By preferentially selecting individuals with large crowding distances, the calculation results can be uniformly distributed in the target space to maintain the diversity of the population.

d: SELECTION AND RECOMBINATION

The generated children population is reorganized with the parent population, retaining elite individuals in their respective populations and passing them on to the next generation. Based on nondominated sorting and individual crowding distances, inferior individuals are eliminated until the current population size is met.

(5) Crossover and mutation

Simulated binary crossover is shown below.

$$c_{1,k} = \frac{1}{2}\left[(1 - \beta_k) p_{1,k} + (1 + \beta_k) p_{2,k}\right] \tag{25}$$

$$c_{2,k} = \frac{1}{2}\left[(1 + \beta_k) p_{1,k} + (1 - \beta_k) p_{2,k}\right] \tag{26}$$

where $c_{i,k}$ is the i^{th} child's k^{th} component and $p_{i,k}$ is the selected parent. $\beta_k(\geq 0)$ is calculated as follows:

$$p(\beta) = \frac{1}{2}(\eta_c + 1)\beta^{\eta_c}, \quad \text{if } 0 \leq \beta \leq 1 \tag{27}$$

$$p(\beta) = \frac{1}{2}(\eta_c + 1)\frac{1}{\beta^{\eta_c+2}}, \quad \text{if } \beta > 1 \tag{28}$$

where η_c is the distribution index for crossover. If u is between (0,1),

$$\beta_u = (2u)^{\frac{1}{(\eta+1)}} \tag{29}$$

$$\beta_u = \frac{1}{[2(1-u)]^{\frac{1}{(\eta+1)}}} \tag{30}$$

and simulated binary crossover is complete. Next, carry out polynomial mutation:

$$c_k = p_k + \left(p_k^u - p_k^l\right)\delta_k \tag{31}$$

where c_k is the child, p_k is the parent, and p_k^u and p_k^i are the upper bound and lower bound of the parent component, respectively. δ_k is a small variation, which is calculated from a polynomial distribution by using

$$\delta_k = (2r_k)^{\frac{1}{\eta m+1}} - 1, \quad \text{if } r_k < 0.5 \tag{32}$$

$$\delta_k = 1 - [2(1-r_k)]^{\frac{1}{\eta m+1}}, \quad \text{if } r_k \geq 0.5 \tag{33}$$

where r_k is a uniformly sampled random number within (0,1) and η_m is the mutation distribution index.

To obtain the compromise solution of the objective function from the Pareto optimal solution output by NSGA-II, the following membership function [27], [28] is established:

$$\mu_i(k) = \begin{cases} 1 & F_i(k) \leq \delta_i \\ \dfrac{F_{i\max} - F_i(k)}{F_{i\max} - \delta_i} & \delta_i < F_i(k) < F_{i\max} \\ 0 & F_{i\max} < F_i(k) \end{cases}$$

$$i = 1, 2 \quad \text{and } k = 1, 2 \cdots P$$

$$\delta_i = F_{i\max} - \theta_i(F_{i\max} - F_{i\min})\, 0 \leq \theta_i \leq 1 \tag{34}$$

where F_{imax} and F_{imin} represent the maximum and minimum values of the two objective functions, respectively. P is the number of Pareto optimal solutions, and μ_i is the membership value of each solution corresponding to the objective function.

θ_i can be adjusted in real time according to the speed of the vehicle and the actual working conditions of the road. At the same time, the selection of the θ_i value affects the choice of the compromise solution. When $\theta_1 = 1, \theta_2 = 0$, choose the compromise solution with the minimum input power; when $\theta_1 = 0, \theta_2 = 1$, choose the compromise solution with the minimum tire load rate; when $\theta_1 = 1, \theta_2 = 1$, choose a compromise solution with the minimum input power and minimum tire load rate.

$$\mu_T(k) = \frac{\mu_1(k) + \mu_2(k)}{\sum_i^P (\mu_1(i) + \mu_2(i))} \quad k = 1, 2 \cdots P \tag{35}$$

The above formula is an aggregate function of two membership functions; the μ_T value of each Pareto optimal solution is calculated, and the largest μ_T value is selected as the compromise solution.

Assume that the initial speed of the vehicle is 50 km/h and that the acceleration is 0.1 g. The relationship between the two objective functions when driving on a favorable road surface is shown in Fig. 6.

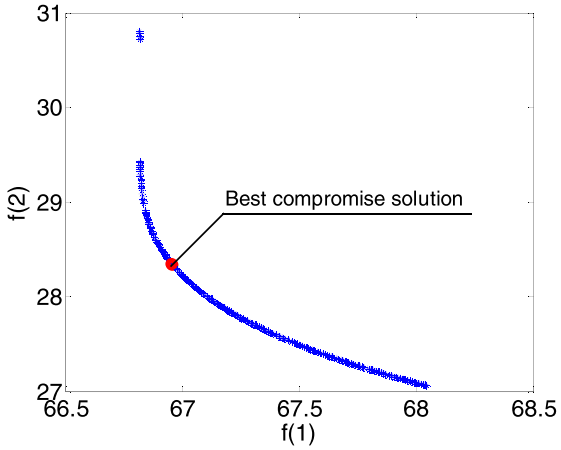

FIGURE 6. Best compromise solution of the Pareto-optimal solution in the example.

Where f(1), f(2) represent the objective functions that characterize the optimization of the drive system efficiency and the optimization of the vehicle driving safety, respectively. The red point represents the best compromise solution of the objective functions because the value of the sum function of the two objective functions is the largest at this point.

2) HYBRID GENETIC TABU SEARCH ALGORITHM

a: GENETIC ALGORITHM

The GA [29] is a parallel, efficient, global search method that simulates the genetic and evolutionary processes of biological systems in the natural environment. It uses only the fitness function values transformed from the objective function values to determine further search directions and search ranges without the need for other auxiliary information, such as the derivative value of the objective function. Relative to conventional optimization algorithms, the obstacle of function derivation is avoided, which makes the genetic algorithm highly advantageous. In recent years, with the rise of artificial intelligence, the development of GAs has been very rapid, particularly in the field of multi-objective optimization. The algorithm starts with a randomly generated population, and the individuals in the population are described by two-level strings. The number of binary strings m_j is calculated by the following formula:

$$2^{m_j - 1} < (b_j - a_j) \times 10^i \leq 2^{m_j} - 1 \tag{36}$$

where a_j and b_j represent the upper and lower bounds of the individual constraint range, respectively, and i is the required precision.

The decimal value of the individual p_j is returned from the binary string using the following formula:

$$p_j = a_j + decimal(substring_j) \times \frac{b_j - a_j}{2^{m_j} - 1} \tag{37}$$

where decimal(substring$_j$) represents the decimal value of the individual p_j.

The evaluation objective function is determined, and the objective function value is converted into the fitness value. In addition, a selection operator is used to select superior individuals from the current population to carry over to the next generation. ''Roulette wheel selection,'' one of the earliest selection methods used in the genetic algorithm, was proposed by Holland. Because it is simple and practical, it is widely used. This is a ratio-based choice, and the selection probability of each individual can be expressed by the following equation:

$$p_j = \frac{f_j}{\sum_{j=1}^{NP} f_j} \quad (j = 1, 2 \cdots, NP) \tag{38}$$

where NP is the size of the population and f_j is the fitness of individual j.

Furthermore, all individuals in the group are randomly paired off; each pair exchanges part of their chromosomes with a predetermined crossover probability to obtain a new individual that combines the superior characteristics of the parents, and the search capability of the genetic algorithm is greatly improved. Furthermore, each individual in the group changes a certain gene value with a predetermined mutation probability to obtain a new individual. As the evolution progresses, the individuals with lower fitness gradually phase out until the termination condition is met, and the optimal individual is the optimal solution.

Algorithm 1 Nondominated Sorting Algorithm

```
for each q∈M
Sp = Ø
np = Ø
  for each q ∈ M
 if  p < q
     Sp=Sp∪{q}
          else if  q < p:
              np =np+1
     if np = 0
        prank = 1
     F1 =F1∪{p}
i=1
while Fi ≠Ø
Q =Ø
     for each p∈Fi
      for each q∈Sp
np= np − 1
              if np=0
     qrank = i+1
       Q=Q∪{q}
  i=i+1
Fi=Q
```

b: TABU SEARCH (TS) ALGORITHM

The TS algorithm [30] is an intelligent search algorithm that simulates human thinking. That is, people will not search the key location immediately but rather search other locations. If not found, then they search the locations that have been visited. This technique can accommodate any type of objective function and optimization problems under corresponding constraints. Relative to genetic algorithms, TS has flexible memory functions and contempt criteria. By setting a tabu table, the algorithm can be prevented from revisiting the solutions that have been accessed during the most recent iterations, thus preventing loops. In addition, this approach can help algorithms avoid local optimal solutions and turn to other regions of the solution space, thereby increasing the probability of obtaining a better global optimal solution. The specific steps are as follows:

1. Given the tabu search algorithm parameters, the initial solution is randomly generated, and the tabu table is set to an empty set.

2. Determine whether the algorithm condition is satisfied: if yes, the algorithm ends and outputs the optimal solution; otherwise, it continues.

3. The neighborhood function of the current solution is used to generate several neighborhood solutions, and several candidate solutions are determined therefrom.

4. It is evaluated whether the candidate solution satisfies the contempt criterion: if yes, the best state y satisfying the contempt criterion is used instead of x as the new current solution, that is, x=y. Then, the tabu object that entered the tabu table is replaced with the tabu object corresponding to y, which replaces the optimal state with y, and we go to step (6); otherwise, we continue.

5. Determine the tabu attribute of each object corresponding to the candidate solution, select the best state corresponding to the non-tabu object in the candidate solution set as the new current solution, and replace the tabu object that entered the tabu table with the tabu object corresponding thereto.

6. Determine whether the algorithm termination condition is satisfied: if yes, the algorithm ends to output the optimal solution; otherwise, the process proceeds to step 3.

c: HYBRID GENETIC TABU SEARCH ALGORITHM

Based on the group search strategy and simple genetic operators, the genetic algorithm has powerful global search ability, information processing parallelism and application robustness. However, a large number of practices and studies have shown that genetic algorithms have poor local search ability, exhibit a ''premature'' phenomenon, move around in the vicinity of the optimal solution, and exhibit

Algorithm 2 Hybrid Genetic Taboo Search Algorithm

Initialize the parameters, set the maximum evolution algebra G, randomly generate the initial population P of N individuals, establish a fitness function, and empty the taboo table (TT).
for i=1:G
  for j=1:N
    Calculate the fitness values of individual individuals in the population.
  end
 Perform copy, cross, and mutate operations
end
Output the optimal solution as the current solution (CUS) and best-so-far solution (BS) of the taboo search algorithm.
g=1
while g<G
  for i=1:ca
    generate neighborhood solutions (NSs) and determine several candidate solutions (CASs).
  end
  if $f_{CAS} \leq f_{CUS}$
    CUS=CAS, update the TT.
      g=g+1
   else
        if $f_{CAS} \geq f_{CUS}$
        the improved solution (IS) of CAS is assigned to the CUS; update the TT.
      BS=IS
g=g+1
else
      if IS$\notin$TT
          CUS=CAS; update the TT.
      g=g+1
        else
          NS=CUS
       end
      end
  end
end

slow convergence. The tabu search algorithm has strong local search ability. By setting the length of the tabu table reasonably, the loop can be escaped to find the optimal solution. However, there is a strong dependence on the initial solution. A satisfactory initial solution can make the TS search find a better solution in the solution space, while a poor initial solution reduces the convergence speed of the tabu search. In this paper, the advantages of the genetic algorithm and tabu search algorithm are combined, and the HGTSA is proposed. First, the global search ability of the genetic algorithm is used to conduct a global search. The search result is used as the initial solution of the tabu search algorithm, and then the tabu search algorithm is used for a local search to find the optimal solution. The pseudocode is as follows:

IV. SIMULATION AND TEST VALIDATION

In this section, according to the 7-degree-of-freedom vehicle model established in the second section, a simulation analysis is performed on the MATLAB/Simulink software platform to validate the effectiveness of the proposed control strategy. The vehicle parameters used are shown in Table 1:

TABLE 1. Basic parameters of the vehicle.

Variables	Notation	Value	Unit
Vehicle mass	m	1360	kg
Vehicle inertia moment around the z-axis	I_z	1993	kg·m^2
Distance from the front axle to the mass center	a	1.063	m
Distance from the rear axle to the mass center	b	1.485	m
Wheelbase	l_x	1.422	m
Wheel effective radius	R_W	0.3	m
Centroid height	H	0.492	m

A. HIGH-ADHESION ROAD SURFACE NEDC CONDITION SIMULATION

The road surface adhesion coefficient μ is 1, and initial speed of the vehicle is 50 km/h. The NEDC speed mode simulation experiment is performed.

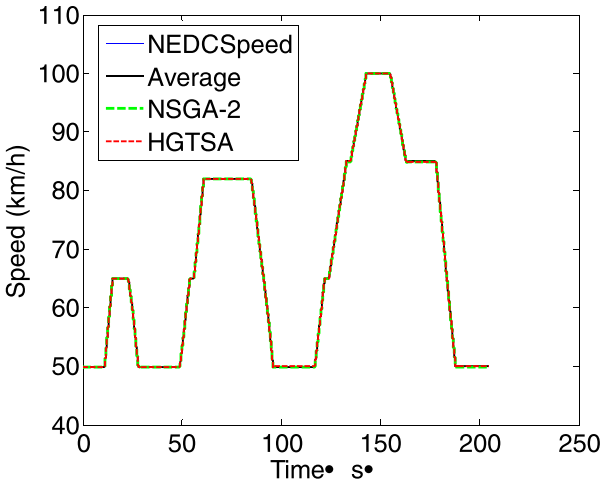

FIGURE 7. Speed response.

Figure 7 shows the speed response, which can be found on the high-adhesion road; the three distribution methods can well track the desired speed.

Figure 8 shows the torque response; when the car is driving at a constant speed, it is mainly driven by the rear axle. By using the HGTSA and the NSGA-II algorithm to optimize the torque distribution, the single-axle drive and the four-wheel drive can be switched according to the demand

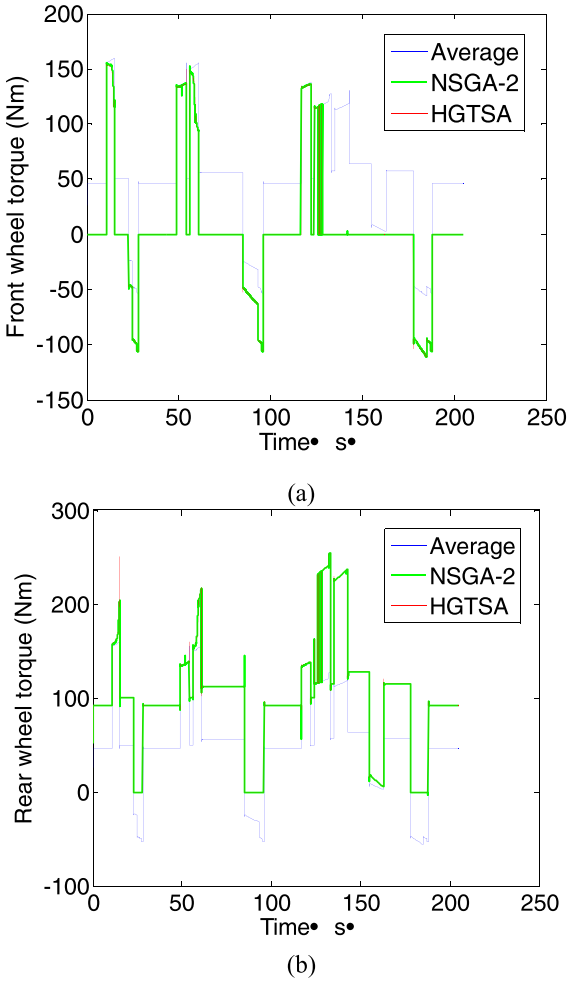

FIGURE 8. Torque response.

torque, but the front and rear wheel torques distributed by the two optimization algorithms are not much different.

Figure 9 shows the energy efficiency response, indicating that the results of the HGTSA and NSGA-II algorithm to optimize the torque distribution, front- and rear-axis motor efficiency and system drive efficiency are almost the same and are much higher than the average distribution. Figure 9d shows that the energy consumption of the optimized vehicle after distribution is less than the average distribution.

Figure 10 shows the distribution of the motor operating points, and Figure 10a shows a distribution diagram of the average distributed motor operating point. Most of the operating points fall within the motor efficiency range of 0.6-0.8, and the motor working capacity is not fully utilized. Figure 10b and 10c present a distribution diagram of the operating point of the motor using the NSGA-II and HGTSA algorithms to optimize the torque distribution. The proportion of the front-axle motor and the rear-axle motor falling within the range of the motor efficiency greater than 0.8 is greatly increased. Both optimization algorithms fully exploit the working potential of the motor to improve the efficiency of the drive system.

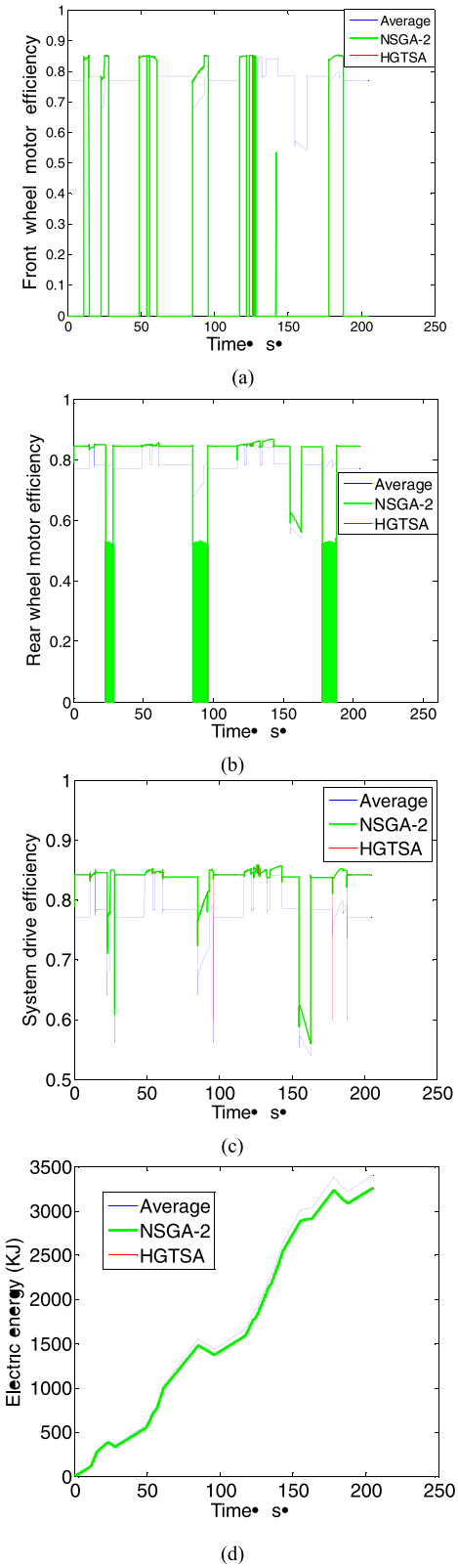

FIGURE 9. Energy efficiency response.

The performance indicators on the high-adhesion road surface coefficient experiment are shown in Table 2.

According to the results of Table 2, the ratio of the motor efficiency that is greater than 0.8 after the torque

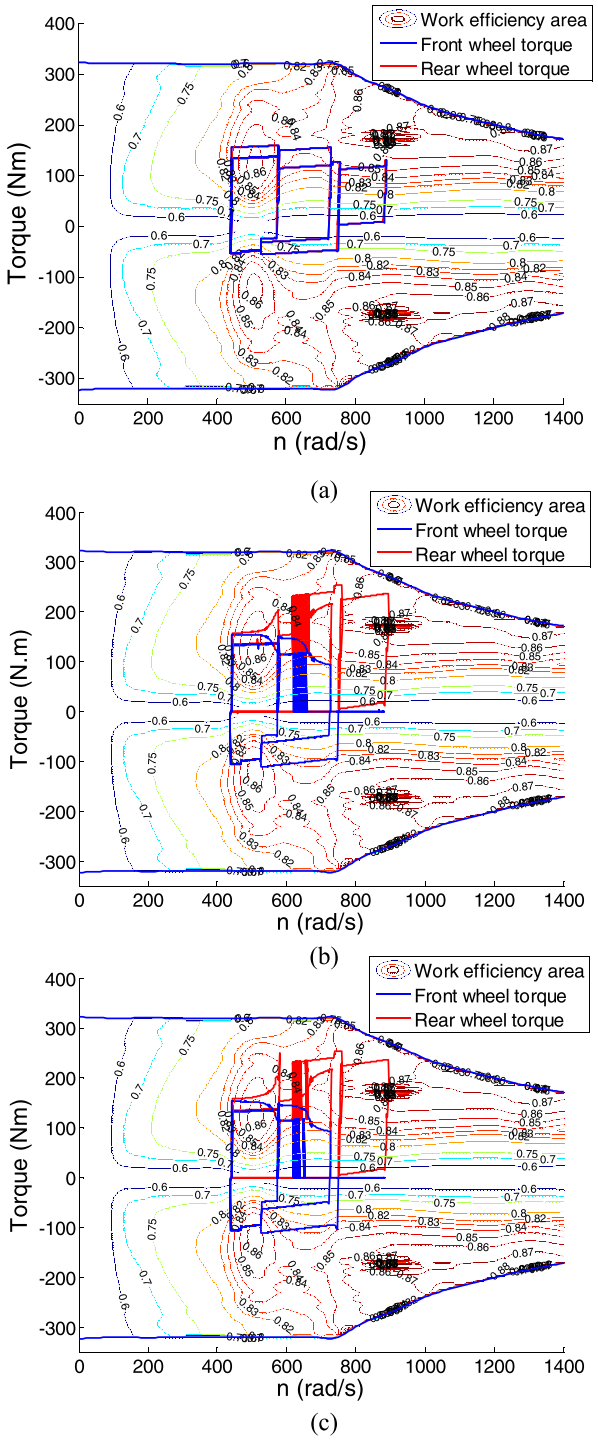

FIGURE 10. Motor operating point distribution diagram. (a) Average. (b) NSGA-II. (c) HGTSA.

distribution using the HGTSA is 94.27%, which is only 0.04% above the ratio of 94.23% after the torque distribution using the NSGA-II algorithm. This value is much larger than the ratio of the average distributed motor efficiency, which is 16.13%. There is almost no difference in the vehicle consumption after the two optimization algorithms perform torque distribution. The energy consumed by the HGTSA for

TABLE 2. Performance indicators on high-adhesion roads.

Torque distribution method	Energy consumption (kJ)	Ratios_0.8
Average distribution	3410.14	16.13%
Allocation by NSGA-Ⅱ	3260.54	94.23%
Allocation by HGTSA	3259.20	94.27%

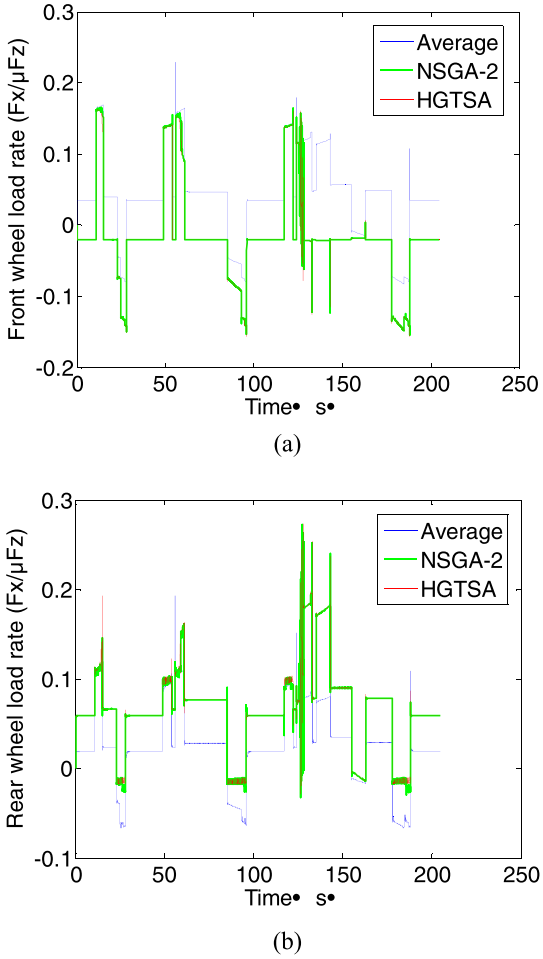

FIGURE 11. Tire load rate.

torque distribution is reduced by 150.94 kJ relative to the average allocated energy consumption, which is only 1.34 kJ less than the energy consumed by the NSGA-II algorithm for torque distribution.

Figures 11 and 12 show the tire load rate and wheel slip rate, respectively. The results of torque distribution using the HGTSA optimization algorithm are close to those obtained using NSGA-II for torque optimization. However, from the front-wheel load factor and the rear-wheel load rate of Figures 11a and 11b, when the car is running at a constant speed, the front- and rear-wheel load rates are smaller than

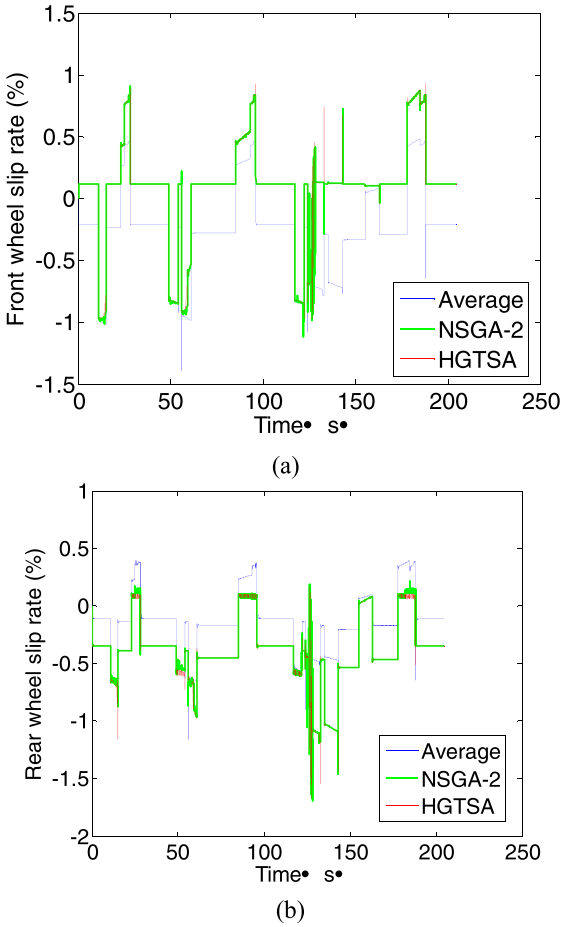

FIGURE 12. Wheel slip rate.

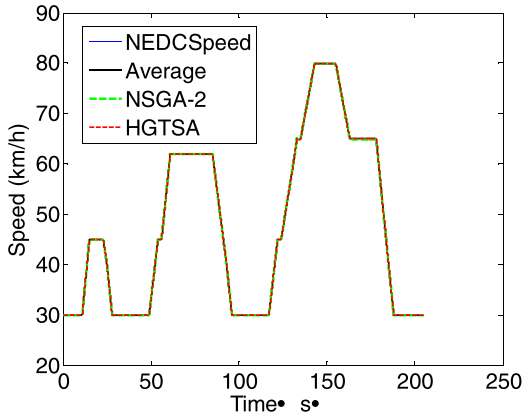

FIGURE 13. Speed response.

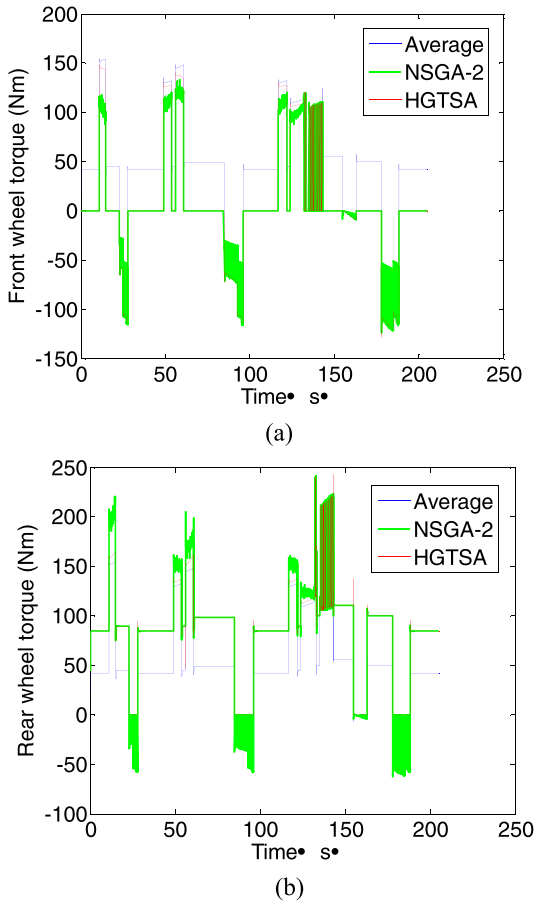

FIGURE 14. Torque response.

the average distribution. The longitudinal safety margin of the car is higher. As shown in Figure 12a, the front wheel is always in a slip-and-roll state and is only in a slip-and-move state when the car accelerates. Although Figure 12b shows the rear wheel slipping in a slip-and-move state at constant speed and acceleration, the slip ratio does not exceed 1.5%.

B. LOW-ADHESION ROAD SURFACE NEDC CONDITION SIMULATION

The road surface adhesion coefficient μ is 0.4, and the initial vehicle speed is 30 km/h. The NEDC working condition simulation experiment is carried out.

Figure 13 shows the speed response. On low-adhesion roads, the three distribution methods also track the desired speed very well.

Figure 14 shows the torque response, which optimizes the torque distribution convergence on the low-adhesion road using the NSGA-II algorithm. When the car accelerates or decelerates, it frequently switches between single-axis drive and four-wheel drive, which affects the ride comfort to some extent.

Figure 15 shows the energy efficiency response. The HGTSA is better than the NSGA-II algorithm for optimizing the torque distribution. Moreover, according to the vehicle energy consumption curve of Figure 15d, the energy consumption of the torque distributed by NSGA-II is larger than the average distribution due to the frequent switching of the operating mode of the motor.

Figure 16 shows the motor operating point distribution, and Figure 16b shows a motor operating point distribution that optimizes torque distribution using NSGA-II. The motor

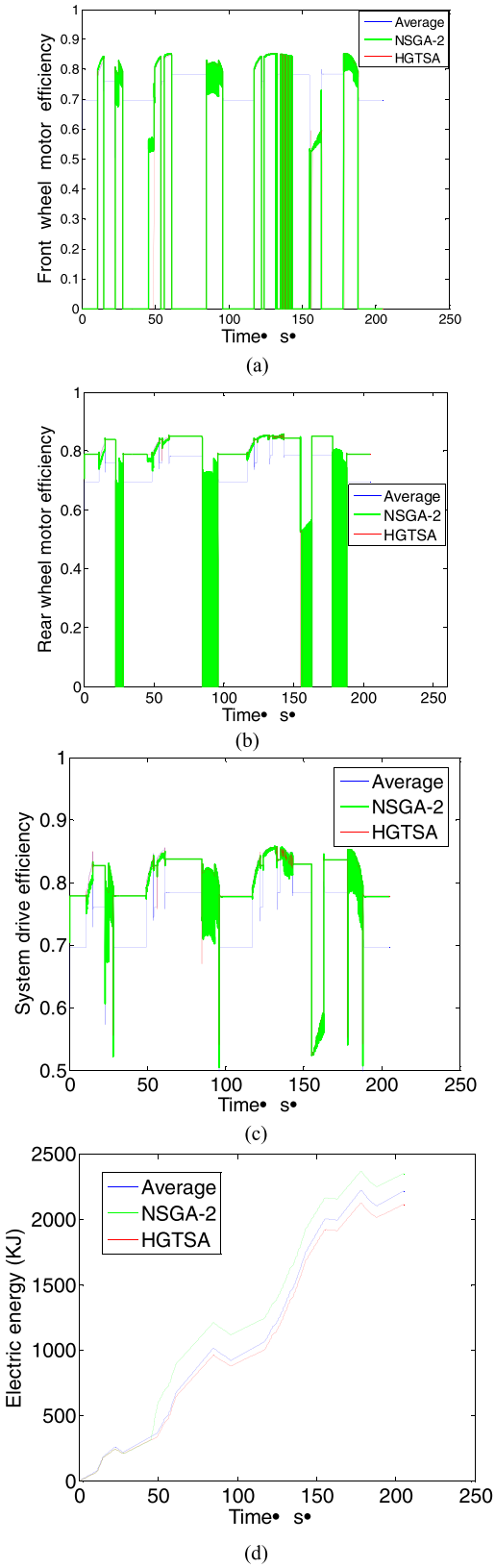

FIGURE 15. Energy efficiency response.

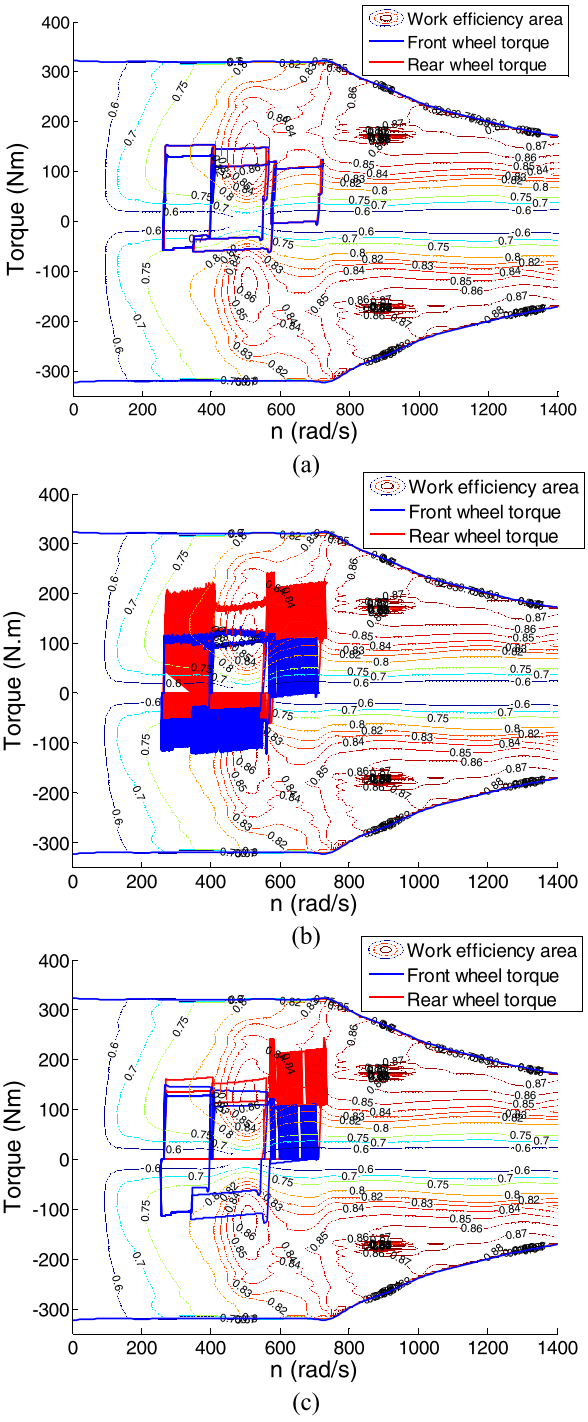

FIGURE 16. Motor operating point distribution. (a) Average. (b) NSGA-II. (c) HGTSA.

has more operating points than the average distribution and optimization of torque distribution using the HGTSA because the simulation uses a variable step size. Figure 16c uses the HGTSA to optimize torque distribution. Fast convergence is achieved, and most of the operating points fall within the range where the motor efficiency is greater than 0.8.

The performance indicators on the low-adhesion-coefficient road surface experiment are shown in Table 3.

According to the comparison of the results in Table 3, the ratio of motor working efficiency greater than 0.8 after

TABLE 3. Performance indicators in a low-adhesion setting.

Torque distribution method	Energy consumption (kJ)	Ratios_0.8
Average distribution	2220.36	13.42%
Allocation by NSGA-Ⅱ	2355.01	40.90%
Allocation by HGTSA	2118.56	49.38%

using the HGTSA to optimize torque distribution is 49.38%, which is 8.48% higher than using NSGA-II. The torque distribution is increased by 35.96% over the average value.

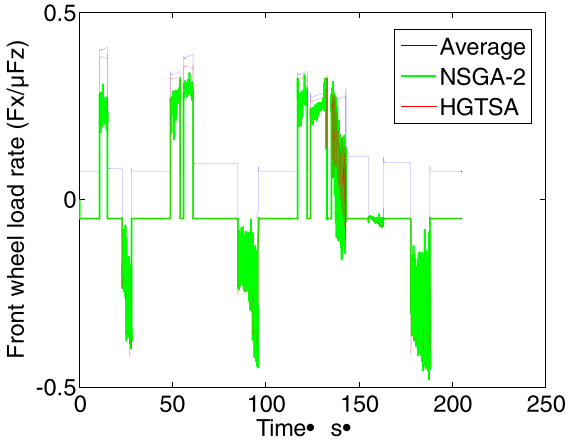

(a)

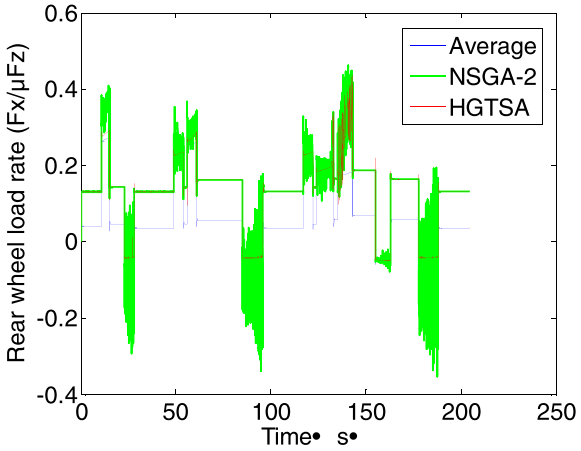

(b)

FIGURE 17. Tire load rate.

Figures 17 and 18 show the tire load rate and wheel slip rate, respectively. From Figure 17a, when the vehicle is running at a constant speed, the front-axle load rate after optimizing the torque distribution using NSGA-II and

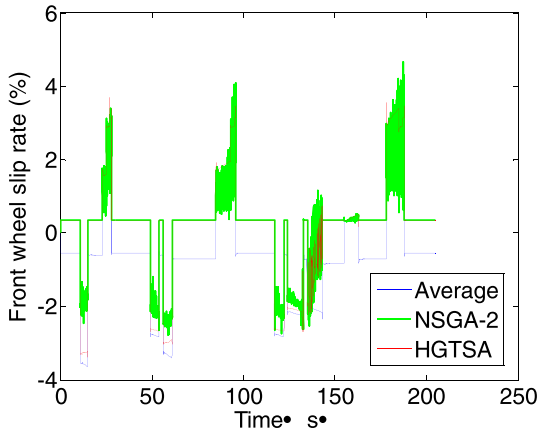

(a)

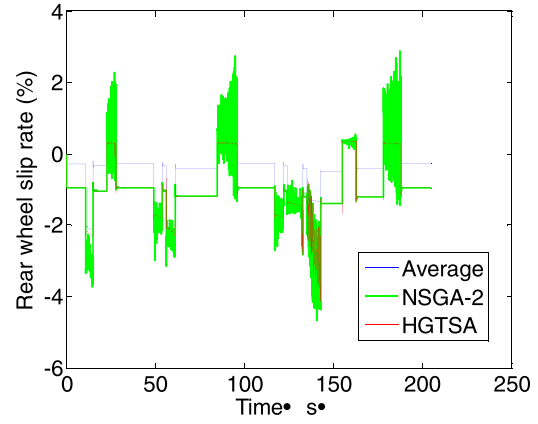

(b)

FIGURE 18. Wheel slip rate.

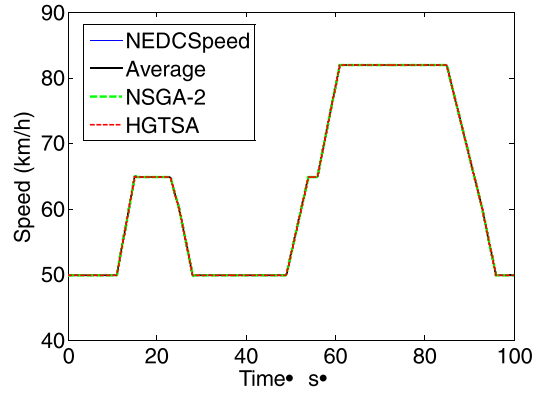

FIGURE 19. Tire load rate.

the HGTSA is always lower than the average distribution. Nevertheless, the rear-axle load rate is increased, particularly when the car accelerates or decelerates in Figure 17b. Figure 18a shows the front-wheel slip rate, which slips only when the car is accelerating. However, the rear-wheel slip ratio as shown in Figure 18b, although always in a slip state, does not exceed 4%. On the low-adhesion road surface,

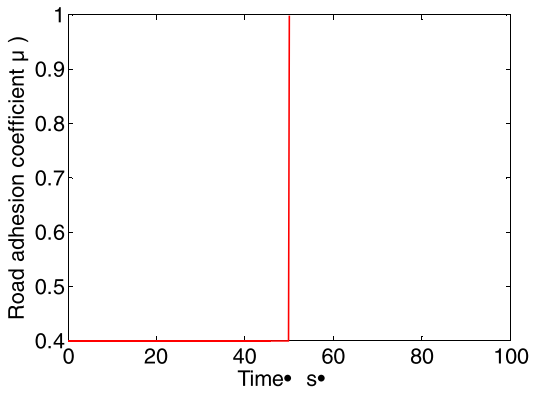

FIGURE 20. Road adhesion coefficient.

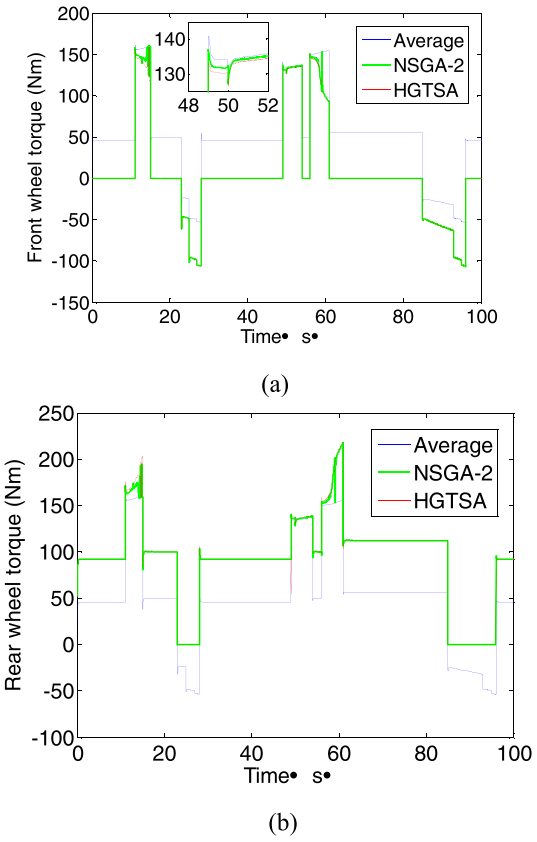

FIGURE 21. Torque response.

the HGTSA is used to optimize the torque distribution to improve the efficiency of the drive system and ensure driving safety at the same time. Relative to NSGA-II, the oscillation is small near the optimal distribution torque value, and the convergence effect is satisfactory.

C. NEDC CONDITION SIMULATION UNDER A CHANGING-ADHESION ROAD SURFACE

The road surface adhesion coefficient μ is variable, and the initial vehicle speed is 50 km/h. The NEDC working condition simulation experiment is carried out.

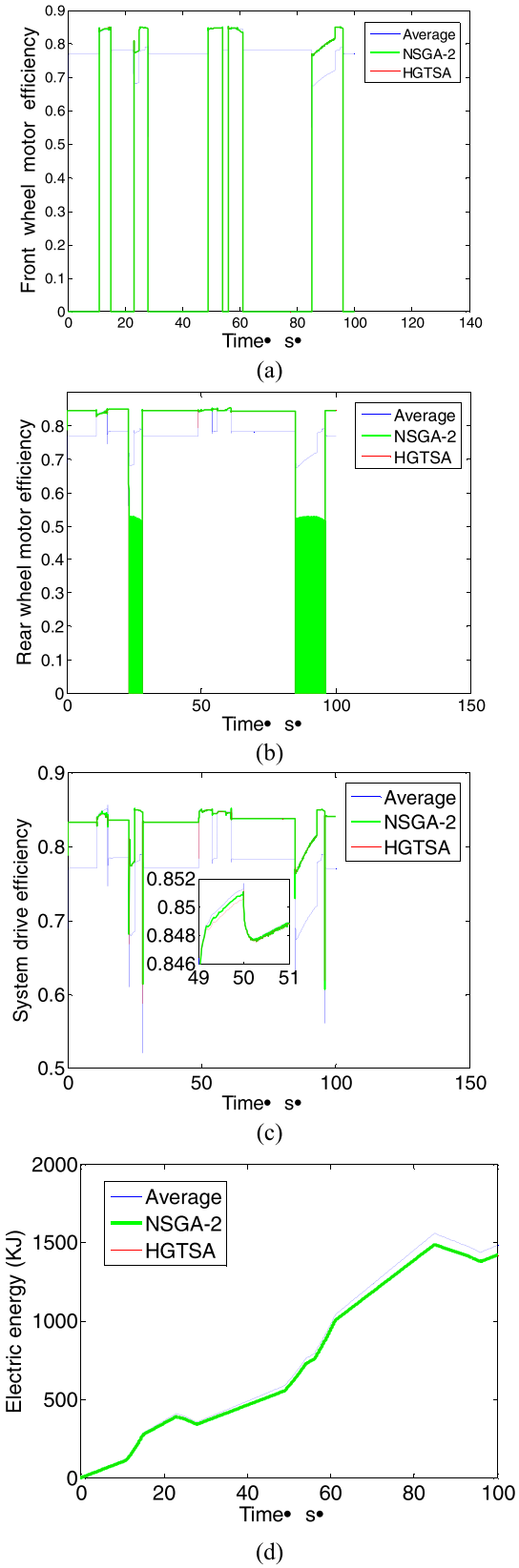

FIGURE 22. Energy efficiency response.

Figure 19 shows the speed response, which indicates that the three distribution methods can also well track the desired speed on the road with changing adhesion.

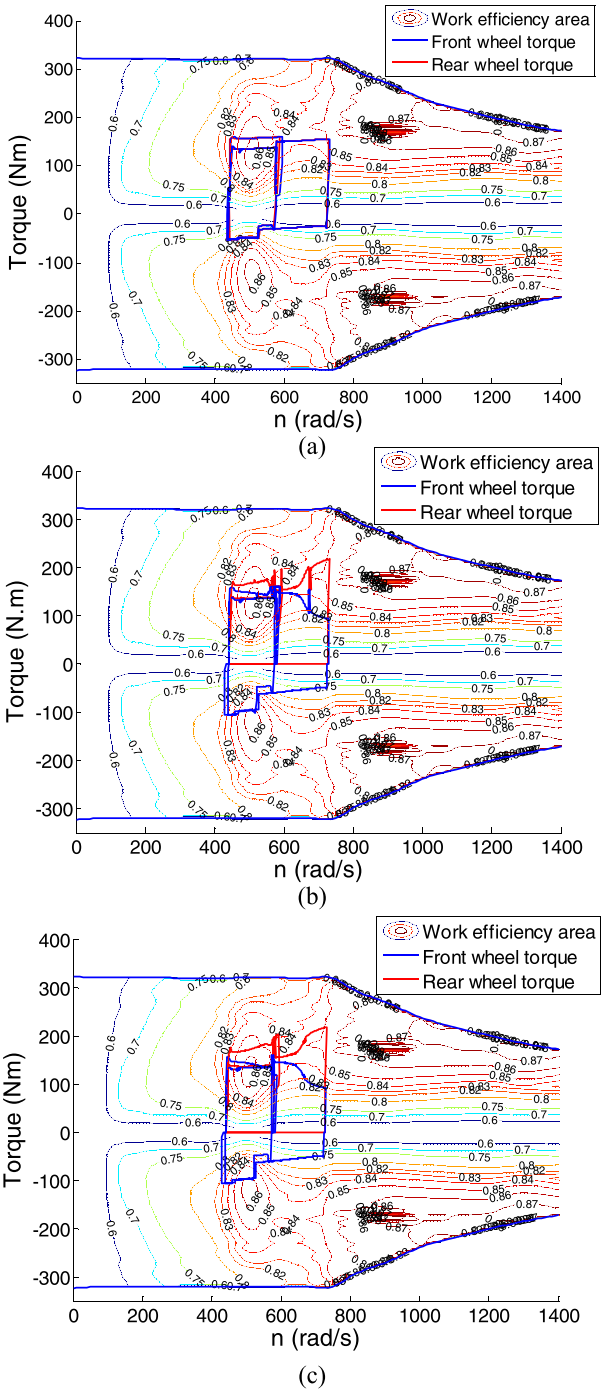

FIGURE 23. Motor operating point distribution. (a) Average. (b) NSGA-II. (c) HGTSA.

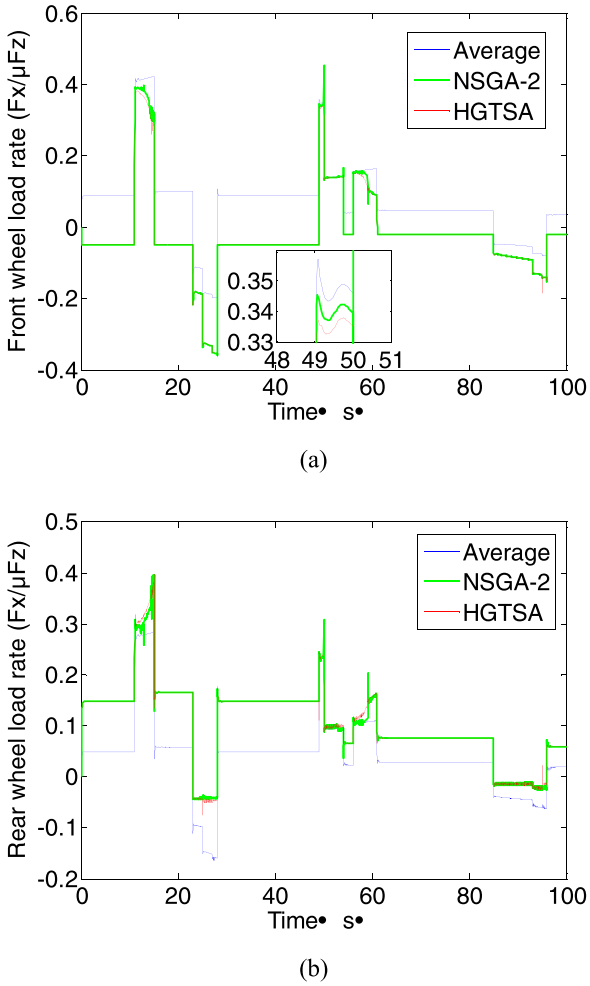

FIGURE 24. Tire load rate.

Figure 20 shows the road adhesion coefficient has a step when time is 50 seconds. The road surface adhesion coefficient μ is 0.4 before 50 seconds; after 50 seconds, the road adhesion coefficient is 1.

Figure 21a and 22c show that using the HGTSA is better than using the NSGA-II algorithm to optimize the torque distribution when the road adhesion coefficient changes from 0.4 to 1. In addition, when the vehicle is driving on the high-adhesion or low-adhesion road surface, the simulation results are the same as those of experiment A and experiment B.

As shown in Figure 23b and 23c, the result of using NSGA-II and the HGTSA to optimize the torque distribution are the same because the simulation time is too short and the data sampling points are too small. However, both of the optimization algorithms fully exploit the working potential of the motor than average distribution.

The performance indicators on the changing-adhesion-coefficient road surface experiment are shown in Table 4.

There is almost no difference in the vehicle consumption by using two optimization algorithms to optimize torque distribution. However, the ratio of the motor efficiency is greater than 0.8, which is far greater than average distribution. In addition, the energy consumed by the HGTSA for torque distribution is reduced by 74.6 kJ relative to the average allocated energy consumption.

Figures 24 and 25 show the tire load rate and wheel slip rate, respectively. When the road adhesion coefficient changes from 0.4 to 1, as shown in Fig. 24a, the front wheel

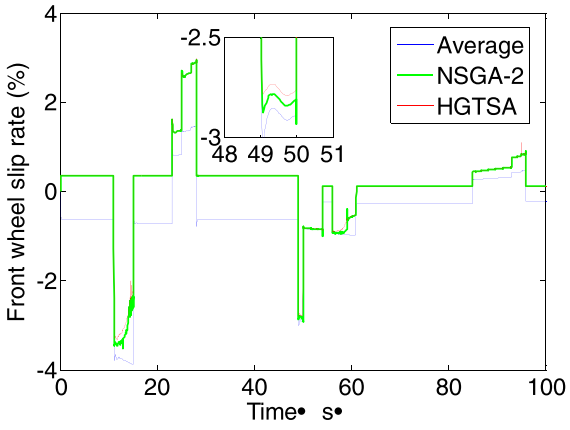

(a)

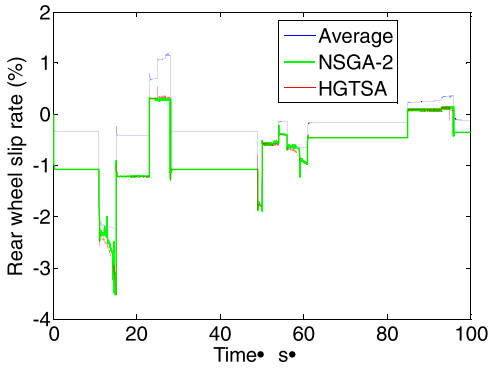

(b)

FIGURE 25. Wheel slip rate.

TABLE 4. Performance indicators under low-adhesion conditions.

Torque distribution method	Energy consumption (kJ)	Ratios_0.8
Average distribution	1560.2	15.78%
Allocation by NSGA-Ⅱ	1488.6	92.29%
Allocation by HGTSA	1488.1	92.36%

tire road rate after optimizing the torque distribution using the HGTSA is smaller than that using NSGA-II and the average distribution. As shown in Fig. 25a, the front wheel slip rate is also the smallest by using the HGTSA to optimize the torque distribution.

V. CONCLUSIONS

This paper proposes a multi-objective optimization method based on torque allocation optimization, which improves the longitudinal driving safety and driving system efficiency of distributed electric drive vehicles. The key contributions include the following:

1) The response surface method is used to perform regression analysis on the test data of the drive motor to obtain the drive motor efficiency function.
2) The optimal torque distribution of the distributed electric drive system is obtained, and the HGTSA and NSGA-II are proposed to solve the multi-objective optimization problem.
3) The NEDC operating conditions are selected to verify NSGA-II, the HGTSA and commonly used average distribution methods. The simulation results show that NSGA-II and the HGTSA can improve the driving efficiency and vehicle driving safety of distributed electric drive systems relative to the average distribution method. In particular, the optimization effect of the HGTSA is more prominent, and stability is achieved more quickly.

REFERENCES

[1] A. M. Andwari, A. Pesiridis, S. Rajoo, R. Martinez-Botas, and V. Esfahanian, "A review of battery electric vehicle technology and readiness levels," *Renew. Sustain. Energy Rev.*, vol. 78, pp. 414–430, Oct. 2017.
[2] E. L. Olson, "Lead market learning in the development and diffusion of electric vehicles," *J. Cleaner Prod.*, vol. 172, pp. 3279–3288, Jan. 2018.
[3] T. Liu and X. Hu, "A bi-level control for energy efficiency improvement of a hybrid tracked vehicle," *IEEE Trans. Ind. Informat.*, vol. 14, no. 4, pp. 1616–1625, Apr. 2018.
[4] T. Liu, X. Hu, S. E. Li, and D. Cao, "Reinforcement learning optimized look-ahead energy management of a parallel hybrid electric vehicle," *IEEE/ASME Trans. Mechatronics*, vol. 22, no. 4, pp. 1497–1507, Aug. 2017.
[5] C. M. Martinez, X. Hu, D. Cao, E. Velenis, B. Gao, and M. Wellers, "Energy management in plug-in hybrid electric vehicles: Recent progress and a connected vehicles perspective," *IEEE Trans. Veh. Technol.*, vol. 66, no. 6, pp. 4534–4549, Jun. 2017.
[6] H. Jiang, H. Zhao, K. Huang, and F. Liu, "A simulation study on the shift schedule of electric vehicle aiming at fuel economy," *Automot. Eng. (Chin. J.)*, vol. 37, no. 7, pp. 819–824. Jul. 2015.
[7] Z. Yu, L. Zhang, and L. Xiong, "Optimized torque distribution control to achieve higher fuel economy of 4WD electric vehicle with four in-wheel motors," *J. Tongji Univ.*, vol. 33, no. 10, p. 1355, 2005.
[8] D. Xu, G. Wang, B. Cao, and X. Feng, "Study on optimizing torque distribution strategy for independent 4WD electric vehicle," *J. Xi'an Jiaotong Univ.*, vol. 46, no. 3, p. 009, Mar. 2012.
[9] X. Yuan and J. Wang, "Torque distribution strategy for a front- and rear-wheel-driven electric vehicle," *IEEE Trans. Veh. Technol.*, vol. 61, no. 8, pp. 3365–3374, Oct. 2012.
[10] Y. Chen and J. Wang, "Design and experimental evaluations on energy efficient control allocation methods for overactuated electric vehicles: Longitudinal motion case," *IEEE/ASME Trans. Mechatronics*, vol. 19, no. 2, pp. 538–548, Apr. 2014.
[11] Y. Chen and J. Wang, "Energy-efficient control allocation with applications on planar motion control of electric ground vehicles," in *Proc. IEEE Amer. Control Conf. (ACC)*, Jun./Jul. 2011, pp. 2719–2724.
[12] D. Lu, M. Ouyang, J. Gu, and J. Li, "Torque distribution algorithm for a permanent brushless DC hub motor for four-wheel drive electric vehicles," *J. Tsinghua Univ. (Sci. Technol.)*, vol. 4, p. 006, Apr. 2012.
[13] D. Lu, M. Ouyang, J. Gu, and J. Li, "Instantaneous optimal regenerative braking control for a permanent-magnet synchronous motor in a four-wheel-drive electric vehicle," *Proc. Inst. Mech. Eng., D, J. Automobile Eng.*, vol. 228, no. 8, pp. 894–908, 2014.
[14] K. Hartani, M. Bourahla, Y. Miloud, and M. Sekour, "Electronic differential with direct torque fuzzy control for vehicle propulsion system," *Turkish J. Electr. Eng. Comput. Sci.*, vol. 17, no. 1, pp. 21–38, 2009.
[15] Y.-P. Yang and C.-P. Lo, "Current distribution control of dual directly driven wheel motors for electric vehicles," *Control Eng. Pract.*, vol. 16, no. 11, pp. 1285–1292, 2008.

[16] X. Lu, Z. Yu, W. Jiang, and Z. Jiang, "Research on vehicle stability control of 4WD electric vehicle based on longitudinal force control allocation," *J. Tongji Univ. (Natural Sci.)*, vol. 38, no. 3, pp. 417–421, 2010.
[17] L. Xiong, Z. Yu, Y. Wang, C. Yang, and Y. Meng, "Vehicle dynamics control of four in-wheel motor drive electric vehicle using gain scheduling based on tyre cornering stiffness estimation," *Vehicle Syst. Dyn.*, vol. 50, no. 6, pp. 831–846, 2012.
[18] N. L. De, A. Sorniotti, and P. Gruber, "Optimal wheel torque distribution for a four-wheel-drive fully electric vehicle," *SAE Int. J. Passenger Cars-Mech. Syst.*, vol. 6, no. 1, pp. 128–136, 2013.
[19] L. Guo, X. Lin, P. Ge, Y. Qiao, L. Xu, and J. Li, "Torque distribution for electric vehicle with four in-wheel motors by considering energy optimization and dynamics performance," in *Proc. IEEE Intell. Vehicles Symp. (IV)*, Jun. 2017, pp. 1619–1624.
[20] H. R. Baghaee, M. Mirsalim, G. B. Gharehpetian, and H. A. Talebi, "MOPSO/FDMT-based Pareto-optimal solution for coordination of over-current relays in interconnected networks and multi-DER microgrids," *IET Gener., Transmiss. Distrib.*, vol. 12, no. 12, pp. 2871–2886, 2018.
[21] V. Ho-Huu, S. Hartjes, H. G. Visser, and R. Curran, "An improved MOEA/D algorithm for bi-objective optimization problems with complex Pareto fronts and its application to structural optimization," *Expert Syst. Appl.*, vol. 92, pp. 430–446, Feb. 2018.
[22] C. Lin and Z. Xu, "Wheel torque distribution of four-wheel-drive electric vehicles based on multi-objective optimization," *Energies*, vol. 8, no. 5, pp. 3815–3831, 2015.
[23] K. Deb, S. Agrawal, A. Pratap, and T. Meyarivan, "A fast elitist non-dominated sorting genetic algorithm for multi-objective optimization: NSGA-II," in *Proc. Int. Conf. Parallel Problem Solving From Nature*. Berlin, Germany: Springer, 2000, pp. 849–858.
[24] M. Liu, J. Huang, and M. Cao, "Handling stability improvement for a four-axle hybrid electric ground vehicle driven by in-wheel motors," *IEEE Access*, vol. 6, pp. 2668–2682, 2018.
[25] Y. Luo and D. Tan, "Lightweight design of an in-wheel motor using the hybrid optimization method," *Proc. Inst. Mech. Eng., D, J. Automobile Eng.*, vol. 227, no. 11, pp. 1590–1602, 2013.
[26] N. Srinivas and K. Deb, "Muilti-objective optimization using nondominated sorting in genetic algorithms," *Evol. Comput.*, vol. 2, no. 3, pp. 221–248, 1994.
[27] S. Sivasubramani and K. S. Swarup, "Multi-objective harmony search algorithm for optimal power flow problem," *Int. J. Electr. Power Energy Syst.*, vol. 33, no. 3, pp. 745–752, 2011.
[28] S. Sivasubramani and K. S. Swarup, "Environmental/economic dispatch using multi-objective harmony search algorithm," *Electr. Power Syst. Res.*, vol. 81, no. 9, pp. 1778–1785, 2011.
[29] R. Yi, W. Luo, C. Bu, and X. Lin, "A hybrid genetic algorithm for vehicle routing problems with dynamic requests," in *Proc. IEEE Symp. Ser. Comput. Intell. (SSCI)*, Nov./Dec. 2017, pp. 1–8.
[30] D. Pham and D. Karaboga, *Intelligent Optimisation Techniques: Genetic Algorithms, Tabu Search, Simulated Annealing and Neural Networks*. Berlin, Germany: Springer, 2012.

JUHUA HUANG received the B.S. degree in mechanical engineering from Jiangxi Technology University, Nanchang, Jiangxi, China, in 1984, and the M.S. and Ph.D. degrees in material processing engineering from Nanchang University, Nanchang, in 1993 and 1998, respectively.

Since 1998, she has been a Professor with the School of Mechatronics Engineering, Nanchang University. Her main research interests include vehicle system dynamics control and electric vehicle design.

YINGKANG LIU received the B.S. degree in mechatronics engineering from Nanchang University, in 2017, where he is currently pursuing the master's degree with the School of Mechatronics Engineering.

His research interests include vehicle system dynamics modeling and control, trajectory tracking, and path planning for autonomous driving.

MINGCHUN LIU received the B.S. degree in electromechanical engineering and the M.S. and Ph.D. degrees in mechanical engineering from the Beijing Institute of Technology, in 2009, 2010, and 2015, respectively.

Since 2015, he has been an Assistant Professor with the School of Mechatronics Engineering, Nanchang University. Since 2017, he has been a Postdoctoral Researcher with the Department of Mechanical and Aerospace Engineering, The Ohio State University, Columbus, OH, USA. His research interests include electric vehicle system integration, vehicle system dynamics modeling and control, and vehicle control system development.

MING CAO received the degree in software engineering, in 2009, and the M.S. degree in vehicle engineering from Nanchang University, Nanchang, Jiangxi, China, in 2012.

Since 2012, he has been an Assistant Professor with the School of Mechatronics Engineering, Nanchang University, and with the Jiangxi Engineering Research Center of Vehicle Electronics. Since 2017, he has been a Visiting Scholar with the University of Kansas, Lawrence, KA, USA. His main research interest includes battery management system in electric vehicle and vehicle electrical control.

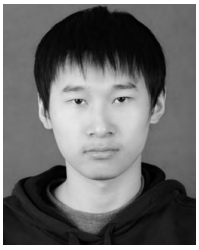

QIHAO YAN received the B.S. and M.S. degrees in logistics engineering from Nanchang University, China, in 2009 and 2015, respectively.

Since 2015, he has been a Junior Engineer with the School of Industrial Engineering, Nanchang University. His research interests include industrial design, engineering control, and logistics management.